Applied Surface Science 623 (2023) 156936

Contents lists available at ScienceDirect

Applied Surface Science

journal homepage: www.elsevier.com/locate/apsusc

Full Length Article

Efficient endoscope inner channel surface disinfection using a two-step atmospheric pressure plasma treatment

Naomi Northage [a], Stéphane Simon [a], Vasyl Shvalya [b], Martina Modic [b], Thorsten Juergens [c], Sascha Eschborn [c], Malcolm J. Horsburgh [d], James L. Walsh [a,e,*]

[a] Centre for Plasma Microbiology, Department of Electrical Engineering and Electronics, University of Liverpool, Liverpool L69 3GJ, UK
[b] Laboratory for Gaseous Electronics, Jožef Stefan Institute, Ljubljana 1000, Slovenia
[c] R&D Endoscopy Reprocessing Systems, Olympus Surgical Technologies Europe, Olympus Winter & Ibe GmbH, Kuehnstraße 61, 22045 Hamburg, Germany
[d] Infection Biology & Microbiomes, Institute of Infection, Veterinary and Ecological Sciences, University of Liverpool, Liverpool L69 7BE, UK
[e] York Plasma Institute, School of Physics, Engineering & Technology, University of York, York YO10 5DQ, UK

ARTICLE INFO

Keywords:
Cold atmospheric plasma
Plasma activated water
Reactive oxygen and nitrogen species
Endoscope reprocessing
Surface damage

ABSTRACT

Flexible endoscopes are ubiquitously used in modern medicine to diagnose and treat a variety of gastrointestinal ailments; however, the inner channels of these complex devices provide an ideal environment for biofilm development. Incomplete or ineffective endoscope reprocessing introduces the potential for cross-contamination between patients, highlighting the need for a new approach to disinfection. In this study, the antibiofilm potential of a two-step disinfection process using cold atmospheric pressure plasma and plasma activated water is considered. It was revealed that the combined approach achieved a 5.72 log reduction of clinically relevant mixed species biofilms from the narrow lumens found within a typical endoscope. To investigate potential surface damage resulting from the decontamination process, the surface composition and morphology were examined using XPS, FTIR and AFM. Following multiple disinfection cycles, few changes to the surface composition or morphology were detected and the corresponding ability of bacteria to adhere on the surface was not enhanced.

1. Introduction

The use of flexible endoscopic devices has become a major feature of modern clinical practice, both for diagnostic applications and surgical interventions [1]. Endoscopic procedures are conducted with thin, tubular reusable devices, the nature of which presents an ideal environment for biofilm development inside the narrow lumens known as the inner channel system of flexible endoscopes [2,3]. Endoscopic procedures are often conducted within non-sterile body cavities exposing the endoscope to the patient's natural microbiota [3,4]. This results in endoscopes becoming heavily contaminated with bioburdens and potentially infectious microorganisms [2,5]. Ensuring endoscopes are safe for patient use involves multiple cleaning steps; including pre-cleaning to prevent biofilm formation, manual cleaning and brushing to remove residual organic material, and high-level disinfection (HLD) [6-8]. Endoscope reprocessing techniques are time-consuming, costly and involve the use of hazardous chemical agents, such as peracetic acid and glutaraldehyde [6,9,10]. Peracetic acid is often used as a preferred method due to its efficiency against a large range of microorganisms and its use results in a reduced amount of protein fixation, preventing build-up of biofilms [2,11]. While development over the past few decades has resulted in the use of automated endoscopes reprocessors (AERs), reprocessing still primarily involves manual cleaning [5]. Standards and recommendations have been developed to ensure suitable disinfection of devices. These are constantly revised and republished; however, reprocessing across sites can differ greatly and deviations from protocols can arise over time. Several studies have highlighted a lack of compliance with established guidelines for endoscope reprocessing [3,12]. While this human error can result in increased risk of infection transmission, flaws in the AER process, delayed reprocessing, incorrect selection or use of disinfectants, and insufficient drying can all contribute [5]. Although rare, reports of patient cross-contamination have risen in recent years, however due to lack of transparency a true estimate of the incidence rate of post-endoscopy infection is lacking [2,13].

There is increasing recognition of the presence of residual microbial contamination in reprocessed patient-ready endoscopes [2,3].

* Corresponding author.
E-mail addresses: jlwalsh@liverpool.ac.uk, james.l.walsh@york.ac.uk (J.L. Walsh).

https://doi.org/10.1016/j.apsusc.2023.156936
Received 25 October 2022; Received in revised form 5 February 2023; Accepted 2 March 2023
Available online 8 March 2023

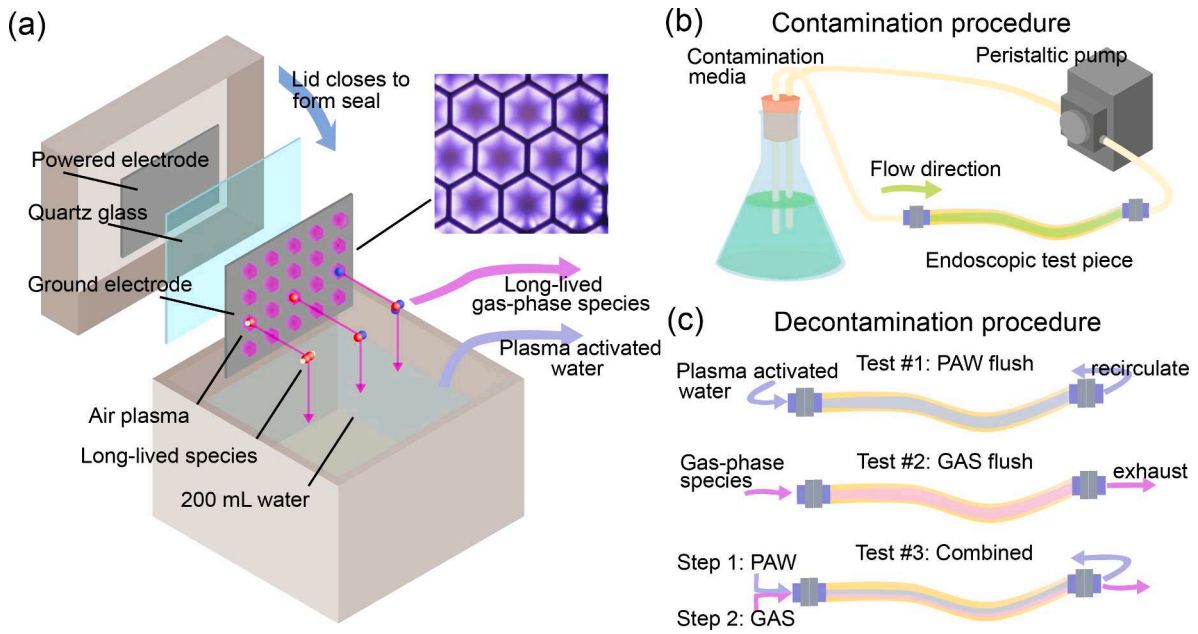

Fig. 1. Experimental setup: (a) schematic of device used for plasma generation and water activation, (b) flow system used to contaminate endoscopic test pieces, and (c) decontamination procedure showing the PAW flush, GAS flush and combined PAW + GAS process.

Reprocessing has therefore come under scrutiny because of infectious outbreaks as a result of multi-drug resistant organisms transmitted by contaminated endoscopes [14]. To ensure HLD of flexible endoscopes, reprocessing involves multiple stages of meticulous cleaning and disinfection followed by drying [6]. Due to the nature of most flexible endoscopes, they are not suitable for heat sterilisation and thus extra care must be taken to ensure complete removal of potentially hazardous microorganisms [6]. Organic contamination from bodily fluids can bind to the inner channels increasing bacterial adherence to the surface and creating a physical barrier shielding microorganisms from HLD [15]. It is likely that multiple cycles of use, disinfection, and cleaning of endoscopes can lead to an accumulation of organic material over time [5,6]. It has been reported that insufficient reprocessing as a result of even the smallest breakdown in protocol can result in a build-up of material within the endoscope encouraging biofilm development [16,17].

Cold atmospheric pressure plasma (CAP) is an emerging disinfection technology that has shown great promise in several applications from food safety to dental disinfection, and is now being applied for wound healing and cancer treatment [18-21]. CAP produces a plethora of reactive oxygen and nitrogen species (RONS), which have been shown to possess antimicrobial, antifungal and antiviral properties [22-24]. Several studies have highlighted the use of CAP to modify surfaces, introducing antimicrobial characteristics; however, other studies have shown that direct plasma treatment of a surface can cause negative changes in surface topology leading to increased bacterial adhesion [20,25,26]. Plasma activated water (PAW) offers an alternative approach to disinfection that may overcome these issues. PAW is generated via the exposure of water to CAP, creating an acidic solution containing a cocktail of RONS [27-29]. Many studies have demonstrated the antimicrobial potential of PAW, even demonstrating its efficacy after several hours to days in storage [30,31]. The concentration and composition of reactive species present in PAW strongly depends upon the chemical composition of the exposed liquid, the mode of plasma generation, and the distance between the plasma and liquid sample [29]. Several past studies have shown that PAW is able to penetrate and eliminate biofilm contamination, making it an extremely effective and convenient antimicrobial agent [32,33].

This study investigates a unique combined disinfection approach, which exploits both CAP and PAW treatments, to eradicate build-up biofilms representative of those found within the narrow lumens of flexible endoscopes. By combining PAW exposure with the gas phase RONS produced by CAP, herein referred to as GAS; an efficient and effective antibiofilm process has been developed which is suitable for the rapid decontamination of endoscopic devices. To ensure the combined disinfection process causes minimal adverse changes to the surface of the endoscope channels AFM, FTIR and XPS were used to probe the morphology and composition of the exposed surface after multiple disinfection cycles.

2. Materials and methods

2.1. Bacterial strains and cultivation

The following bacterial strains were chosen based on their association with endoscopic contamination: methicillin-resistant *Staphylococcus aureus USA300 JE2*, *Staphylococcus epidermidis 1457*, *Pseudomonas aeruginosa PA01* and *Escherichia coli Bw25113*. *E. coli* was grown on Luria broth (LB) agar, and *S. aureus, S. epidermidis* and *P. aeruginosa* were grown on Tryptic soy agar (TSA). A single colony from all strains was used to inoculate 10 mL of broth (LB or TSB). Inoculated media was left to incubate overnight at 37 °C, shaking at 210 rpm, then the concentration adjusted by broth dilution to 1×10^6 CFU/mL.

2.2. Plasma device and liquid activation

A low-temperature, surface barrier discharge (SBD) plasma source was positioned above 200 mL of stirred liquid to produce the PAW, shown in Fig. 1(a). During operation a thin layer of plasma was formed within the hexagonal gaps of a grounded mesh stainless steel electrode on the surface of a dielectric material. The mesh electrode was separated from a high voltage copper plate electrode by a 1 mm thick, 100 × 100 mm quartz plate acting as the dielectric barrier. During plasma generation, long-lived RONS including O_3, NO, N_2O and NO_2, were able to traverse the gas gap and reach the liquid interface [29]. At the liquid interface a plethora of chemical reactions take place to form a variety of known antimicrobial agents, such as H_2O_2, HNO_2 and $ONOO^-$ [34,35]. In all cases, PAW was produced using a 25-minute exposure. The SBD was operated at low (12 W) and high (30 W) power to manipulate the

reactive species produced, with low power favouring the production of reactive oxygen species and higher power operation favouring reactive nitrogen species production, as described in previous works [36].The gas phase RONS created by the same SBD device using the same generation conditions were also flushed through the endoscopic test pieces using a small gas pump (1 L/min) to simultaneously dry and disinfect.

2.3. Contamination of endoscopic test pieces

A flow system, shown in Fig. 1(b), was developed to contaminate endoscope surrogate test pieces prepared from translucent polytetrafluoroethylene (Teflon) tubing with 2.0- or 6.0- mm lumen diameter. A well-established contamination method was used with minor modifications [17,37]. Test pieces were each 10 cm long. Prior to contamination, TSB containing 1 % human serum was pumped into the test pieces using a peristaltic pump at a rate of 100 mL/min until filled. This was kept at 37 °C for 24 h to allow attachment of organic matter to the inner surface of the channels, and thus increase bacterial adherence potential. Media was drained from the test pieces and the system rinsed with 200 mL sterile water. Fresh media was inoculated with the cultured strains and circulated through the system using the previously mentioned flow rate for 45 min. The contamination media was drained, the system rinsed with sterile water and cultivated with discharged contamination liquid from a previous stage. The contaminated test pieces were left to incubate for 24 h at 37 °C. The system was again rinsed, and control test pieces removed for analysis of biofilm formation.

2.4. PAW and GAS disinfection

Disinfection of the contaminated test pieces involved circulation of PAW through the flow system at a flow rate of 100 mL/min, or a GAS flush through the flow system at approximately 1 L/min, shown in Fig. 1 (c). A two-step disinfection method was also tested using both PAW and GAS disinfection, with PAW being pumped through the system first followed by a GAS flush. For all disinfection methods, 5 min and 10 min disinfection times were used and compared to control test pieces.

2.5. Optical emission spectroscopy (OES)

OES was used to obtain a qualitative indication of the excited states produced in the plasma layer. Light from the plasma was guided into a spectrometer (Andor Shamrock 500i) via a UV–VIS fibre optic of diameter 200 μm. In all cases, a grating of 600 lines/mm and entrance slit of 100 μm was used. An iCCD camera (Andor iStar 334) was used to capture spectral data using an exposure time of 10 ms which was not synchronized to the plasma generating voltage. Spectral data was created using an accumulation of 100 individual measurements.

2.6. Fourier transform infrared spectroscopy (FTIR)

FTIR was used for characterisation of reactive species between the plasma and liquid, and to provide insight into which reactive species may “activate” the water. To perfrom FTIR measurements, the plasma-generating electrodes were sealed in the box used for water activation and operated under the same conditions as used for gas disinfection. The plasma effluent was drawn from the reactor into a 10-cm path length gas cell and analysed with an FT/IR-4200 spectrometer (JASCO, Tokyo, Japan). A spectral resolution of 2.0 cm^{-1} was used, and each absorption spectrum was acquired over 25 scans.

2.7. Measurement of PAW chemical composition

Spectrophotometric assays (SPECTROstar Nano, BMG LABTECH) were used to measure concentrations of various RONS within the PAW. All measurements were conducted immediately after liquid activation, including pH using a pH probe (Hanna Instruments 9813-6 with pH probe HI-1285-6). Griess reagent (Supelco Ltd, MFCD01866819) was added to the liquid and the concentration of NO_2^- measured by spectrophotometry at 548 nm. The concentration of NO_3^- was also measured using a colorimetric assay based on the interaction of nitrate ions with sodium salicylate (Sigma-Aldrich Ltd, CAS 54–21-7) in a sulfuric acid medium after evaporation and quantified using spectrophotometry at 420 nm. Hydrogen peroxide concentrations in the treated solution were measured according to the protocol described by Dringen *et al.* using the ferrous-xylenol orange assay [38].

2.8. Analysis of biofilm inactivation, biomass, bacterial viability, and intracellular nitrogen

Biofilm inactivation following plasma treatment was determined by the Miles-Misra plating method. Control and treated test pieces were transferred to a 15 mL falcon tube (Appleton Woods Ltd, Birmingham, UK) containing 5 mL of TSB and left shaking for 15 min at 1800 rpm (VXR basic Vibrax®; IKA, Staufen, Germany). Samples from each tube were taken and serially diluted to use for plating on TSA. Plates were left to incubate for 24 h at 37 °C and then colonies counted. Various assays were used to assess the impact of plasma treatments. Crystal violet staining was conducted to measure remaining bacterial biomass. Bacterial metabolic activity was assessed using an MTT assay (Merck KGaA, Darmstadt, Germany) performed according to the manufacturers protocol to investigate cell viability. A 50 μl sample of each biofilm suspension was combined with 50 μl of MTT solution in the well of a microplate. Following 3 h of incubation at 37 °C, 150 μl of MTT solvent was added into each well and left shaking for 15 min. Viability was measured at 590 nm using a microplate reader (SPECTROstar Nano, BMG LABTECH). Intracellular nitrogen was assessed using a nitrite/nitrate assay (Merck KGaA, Darmstadt, Germany) following the manufacturer protocol.

2.9. Surface characterisation

2.9.1. X-ray photoelectron spectroscopy (XPS)

The chemical composition of the endoscopic test pieces was determined by XPS analysis. A TFA XPS spectrometer, produced by Physical Electronics Inc. operating under ultra-high vacuum (10^{-7} Pa) and equipped with a monochromated Al Kα X-ray source (1486.6 eV) was used. The take-off angle of the electron analyser in the XPS spectrometer was 45° with respect to sample surface. Three different locations were analysed on each sample and the data averaged. The XPS spectra were processed using the software MultiPak, Version 9.5.0. Quantification of the surface composition was performed from XPS peak intensities considering the relative sensitivity factors provided by the instrument manufacturer.

2.9.2. Atomic force microscopy (AFM)

The surface roughness and morphology of the endoscopic test pieces was assessed using AFM (Solver PRO, NT-MDT, Russia). Silicon cantilevers with a typical resonant frequency of 240 kHz and a spring constant of 11.8 N/m were used to acquire images in semi-contact mode at room temperature under ambient conditions. The scanning rate was 1.5 Hz. Flattening of the raw images was performed before surface roughness analysis. The average surface roughness was determined from images with an area of 5 μm × 5 μm.

2.9.3. Attenuated total reflectance - fourier infrared transform spectroscopy (ATR-FTIR)

The chemical structures of the endoscopic test pieces were characterised using ATR-FTIR (Spectrum Two, PerkinElmer, USA) following 1x and 5x 5 min plasma treatments at room temperature. Spectra were obtained at a resolution of 4 cm^{-1} with 32 scans per measurement, probing the range of wavelengths from 4000 cm^{-1} to 350 cm^{-1}.

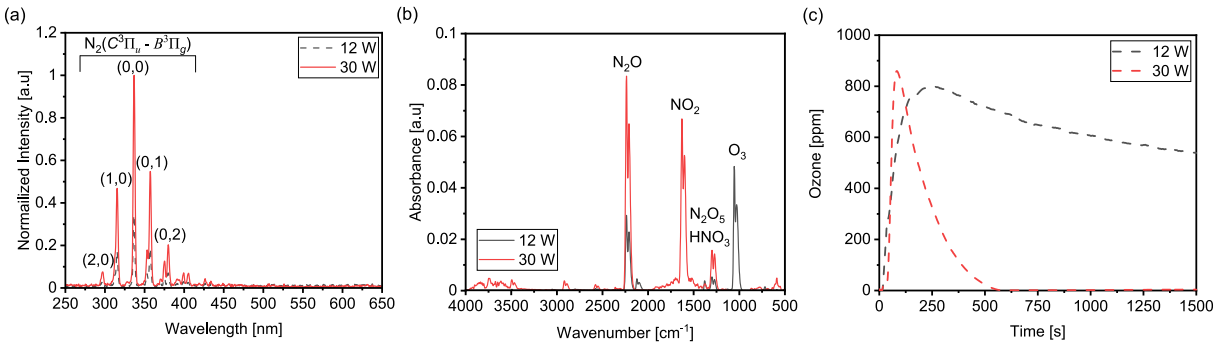

Fig. 2. Gas phase characterisation: (a) Normalised emission intensity from plasma generated after 5 mins of operation at low power (12 W) and high power (30 W) conditions, measured using OES, (b) FTIR absorbance spectra obtained after plasma generation for 5 min at 12 W and 30 W, and (c) Evolution of Ozone concentration measured *in-situ* at a constant dissipated plasma power of 12 W and 30 W.

2.10. Statistical analysis

All experiments were conducted with at least 3 biological repeats and 3 technical repeats. Results are presented as mean or mean ± standard deviation. Statistical analysis was performed using GraphPad Prism 9.0 and OriginPro 2022b. Significance was established using the two-way analysis of variance (ANOVA) test. Due to the nature of the study, a p-value of < 0.05 was considered as significant.

3. Results and discussion

3.1. Plasma and gas phase characteristics

Plasma generation in the humid air between the electrode and liquid surface results in ionisation, excitation, and dissociation reactions of O_2, N_2 and H_2O creating an abundance of reactive species, including O, N, OH, and NO [29,39]. Fig. 2(a) shows the optical emission spectra from the discharge operating at 12 and 30 W; strong emission from the Nitrogen second positive system was observed which is typical of atmospheric pressure air plasma [40]. Beyond the visible plasma region, short-lived species react to form secondary compounds, such as O_3, H_2O_2, NO_2, HNO_2, NO_3 and HNO_3, it is these longer-lived species that diffuse to the liquid interface where they can form NO_2^-, NO_3^- and H_2O_2 [29]. The evolution of reactive species within the gas phase was characterised using FTIR spectroscopy. Fig. 2(b) shows the absorbance spectra of the CAP effluent under 12 W and 30 W operating power after 5 min of generation. Exploration of the absorption spectrum using FTIR showed domination by RNS under higher power conditions, and ROS under lower power generation conditions. A significant ozone peak was detected at around 1056 cm^{-1} when the device was operated at 12 W,

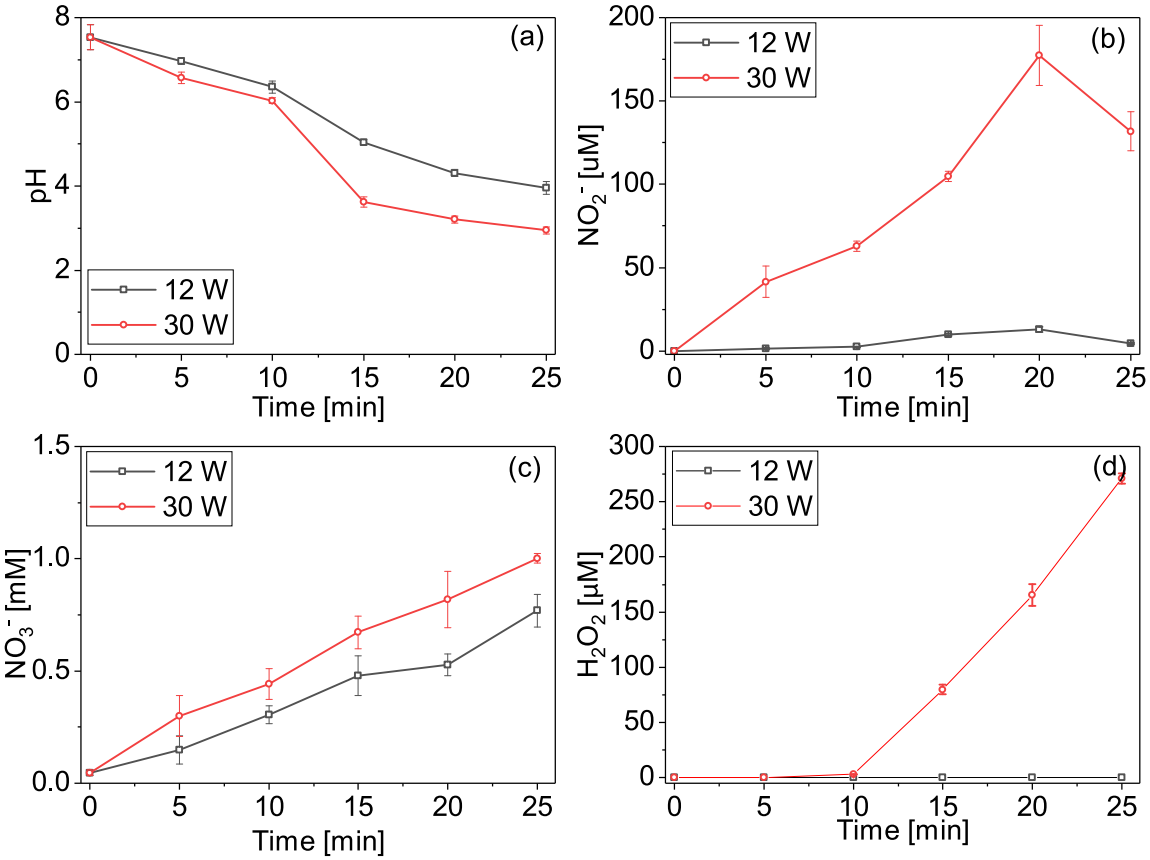

Fig. 3. Kinetic evolution of: (a) pH, (b) nitrite concentration, (c) nitrate concentration, and (d) hydrogen peroxide concentration.

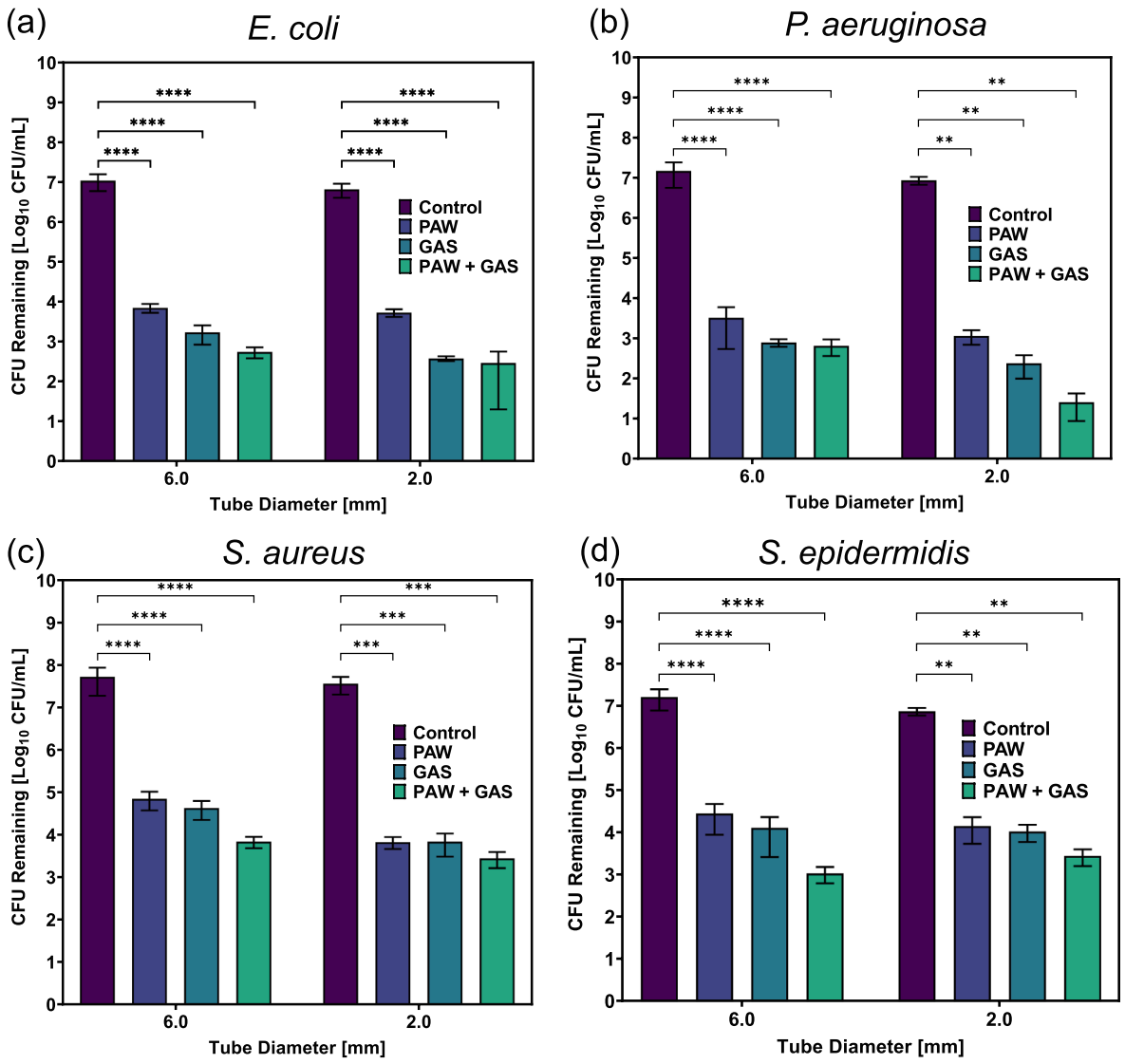

Fig. 4. Effect of 5 min plasma treatment on single species biofilms: (a) *E. coli*, (b) *P. aeruginosa*, (c) *S. aureus*, and (d) *S. epidermidis*.

however minimal ozone was detected by FTIR at an applied power of 30 W. When operated at 30 W prominent peaks were observed for N_2O around 2235 cm^{-1} and NO_2 around 1629 cm^{-1}. In comparison a much smaller peak was found for N_2O at 12 W, and no NO_2 detected. Peaks around 1299 cm^{-1} indicated the presence of N_2O_5 and HNO_3 at both operating powers; however, the peak was smaller for 12 W compared to 30 W indicating a lower concentration. No H_2O_2 was detected within the system. Further ozone quantification, shown in Fig. 2(c) showed a distinct difference between high and low power, with 30 W resulting in a high peak of ozone after 90 s, followed by accelerated quenching. Compared to 12 W which had a high peak after 250 s, followed by a gradual decrease over the duration of the plasma activation. This variation in gas plasma chemistry has been reported by several past studies, which detail the reaction between vibrationally excited N_2 and O found within the discharge forming NO, which readily reacts with O_3 to form NO_2 [25,29].

3.2. Liquid characteristics

During plasma exposure, reactive species in the gas phase diffuse to the water interface where they can either dissolve into solution or react to form other compounds [41,42]. As shown in Fig. 3(a) the pH of the water decreases over the treatment time. This is similar to that observed in other studies using similar plasma devices [43]. It can also be observed that under 12 W CAP generation conditions the decrease in pH was somewhat slower but still resulted in a PAW with a low pH value of 3.95 (±0.15). Many studies attribute the decrease in pH with the formation of nitrites (NO_2^-) and nitrates (NO_3^-) [43,44]. During plasma exposure, reactions between nitrogen oxide compounds, specifically NO_2, and the liquid form nitrites and nitrates, as shown in R1 [43,45].

$$2NO_2 + H_2O \rightarrow NO_2^- + NO_3^- + 2H^+ \quad \text{(R1)}$$

Nitrites further react to form nitrous acid resulting in a decreased pH, and an oxidoreduction reaction occurs in the presence of ozone leading to conversion of nitrites to nitrates:

$$NO_2^- + H^+ \rightarrow HNO_2 \quad \text{(R2)}$$

$$NO_2^- + O_3 \rightarrow NO_3^- + O_2 \quad \text{(R3)}$$

Fig. 3(b) details the kinetic evolution of nitrite within the PAW. Interestingly, past studies have shown that PAW can exhibit a sudden decrease in nitrite concentration to negligible quantities after just a few minutes of plasma exposure, as a result of the conversion of nitrites to nitrates and the use of nitrites for nitrous acid production, resulting in the further acidification of the PAW [43]. However, the nitrite concentration within the PAW in this study continued to increase for 20

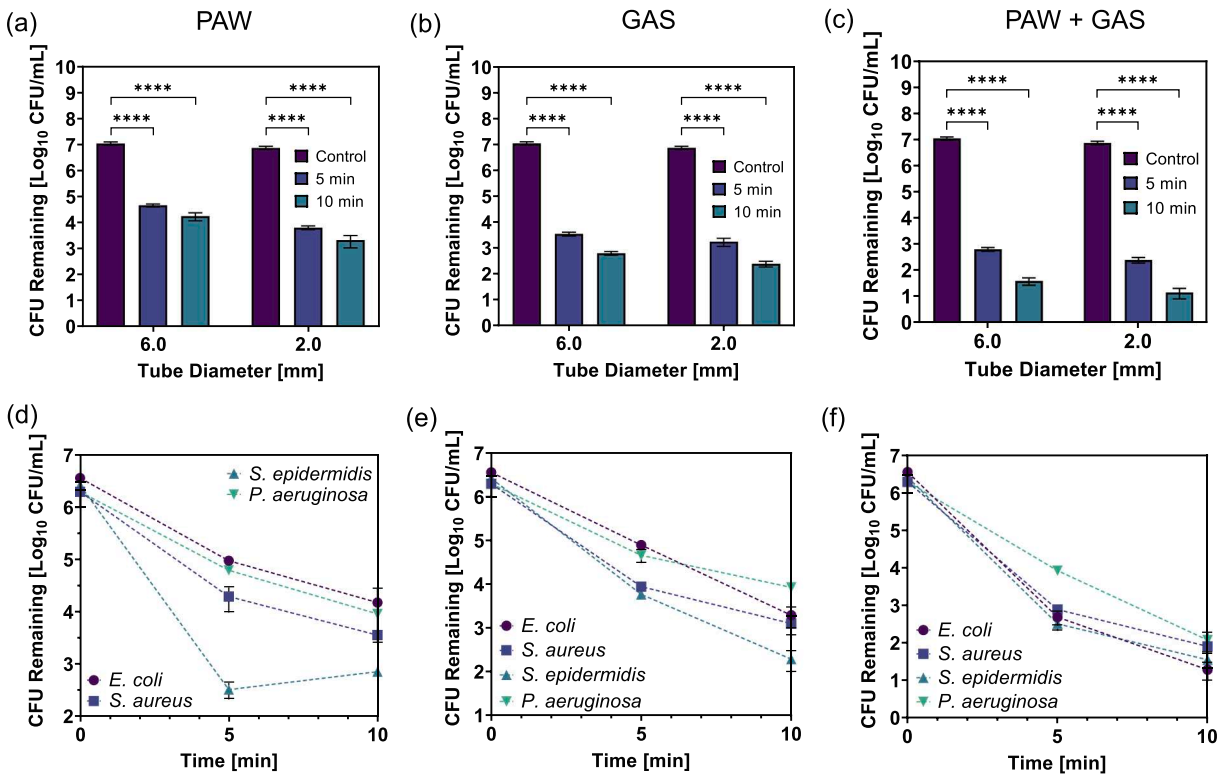

Fig. 5. Effect of 5- and 10- min plasma treatments on mixed species biofilms: (a) PAW treatment, (b) GAS treatment and (c) PAW + GAS treatment. Response to 5- and 10- min plasma treatments across species within the mixed species biofilm: (d) PAW treatment, (e) GAS treatment and (f) PAW + GAS treatment.

min, where it then began to decrease. This phenomenon was previously observed using a similar SBD system and was linked to the generation of NO_3^- in combination with dissolved ozone or via reactions of NO_2^- and H_2O_2 leading to the formation of $ONOO^-$ under acidic conditions [46]. The low power setting produced an effluent dominated by ROS as opposed to RNS which explains the slower increase and significantly lower nitrite concentration (4.56 ± 0.23 uM) compared to the high-power setting (131 ± 11.82 uM). Fig. 3(c) details the kinetic evolution of nitrate within the PAW. Both powers showed a similar linear increase and final concentration for nitrates, 0.77 (±0.07) mM and 1.00 (±0.02) mM, for the 12 W and 30 W case, respectively. The linear increase in concentration has been reported by other studies [29,43,47].

No hydrogen peroxide was detected within the PAW produced with 12 W, while the concentration of H_2O_2 started to increase after 10 min of treatment time when plasma was generated at 30 W as shown in Fig. 3 (d). H_2O_2 can be created in gaseous or aqueous phase via different reactions, however it is commonly assumed that the main reaction responsible for H_2O_2 generation is via OH radical recombination:

$$\dot{O}H + \dot{O}H \rightarrow H_2O_2 \quad \text{(R4)}$$

It is assumed that the presence of these reactive species within the water creates an antimicrobial solution capable of bypassing the complex defence systems present within bacteria by act of simple diffusion [25,48,49]. Preliminary antimicrobial testing (data not shown) demonstrated that PAW generated at 30 W was significantly more effective than PAW generated at 12 W. The reason for this is likely two-fold: (i) a higher operating power produced more gas phase species which ultimately translate into more aqueous phase species; and (ii) a number of previous studies have detailed the link between the dissolution of RNS, which are created in abundance under high power conditions, and antimicrobial activity [50]. Consequently, for all of the antimicrobial and surface analysis tests reported, PAW generated at 30 W was used.

3.3. Effect of plasma treatment on single species biofilms

Single species biofilms of four clinically relevant bacteria: *E. coli*, *S. aureus*, *S. epidermidis*, and *P. aeruginosa*, were formed within endoscopic test pieces following repeated rounds of cultivation and rinsing. Fig. 4 details the colony forming units (CFU) remaining following PAW, GAS and PAW + GAS disinfection. During the disinfection stage PAW was circulated through the flow system and/or GAS flushed through the channels for a total time of 5 min or 10 min. Results showed all plasma treatments were capable of a significant reduction in biofilm contamination. Notably, as shown in Fig. 4(a,b), a 5 min PAW + GAS treatment was capable of achieving a 4.29 and 4.35 log reduction of *E. coli* biofilms and a 4.35 and 5.52 log reduction of *P. aeruginosa* biofilms within lumens of a 6.0 mm and 2.0 mm diameter, respectively. *S. aureus* and *S. epidermidis* showed higher resistance to all plasma treatments, displayed in Fig. 4(c,d); however, a 5 min PAW + GAS treatment still resulted in a 3.88 and 4.11 log reduction in *S. aureus* and a 4.18 and 3.43 log reduction in *S. epidermidis*, for the 6.0 mm and 2.0 mm diameter lumens, respectively. PAW treatment alone resulted in significant log reductions ranging from the lowest at 2.76 for S. epidermidis up to 3.87 for *P. aeruginosa*. While GAS treatment alone resulted in log reductions ranging from 2.85 for *S. epidermidis* to 4.55 for *P. aeruginosa*. *E. coli* and *P. aeruginosa* are Gram-negative bacteria, while *S. aureus* and *S. epidermidis* are Gram-positive bacteria. Several previous studies have shown that Gram-positive species are more resistant to plasma treatments [25,29,51]. Gram-negative bacteria possess a thin peptidoglycan cell wall surrounded by a lipopolysaccharide outer membrane; however, Gram-positive bacteria are surrounded by thicker layers of peptidoglycan instead of the outer membrane [52]. The thicker peptidoglycan layers provide greater protection from environmental stress [51,52]. The greater protection provided by peptidoglycan can be seen from the results with *S. aureus* and *S. epidermidis* proving to be the most resistant to all plasma treatments. *E. coli* is one of the most prevalent microorganisms forming biofilms on medical devices and often used as a model

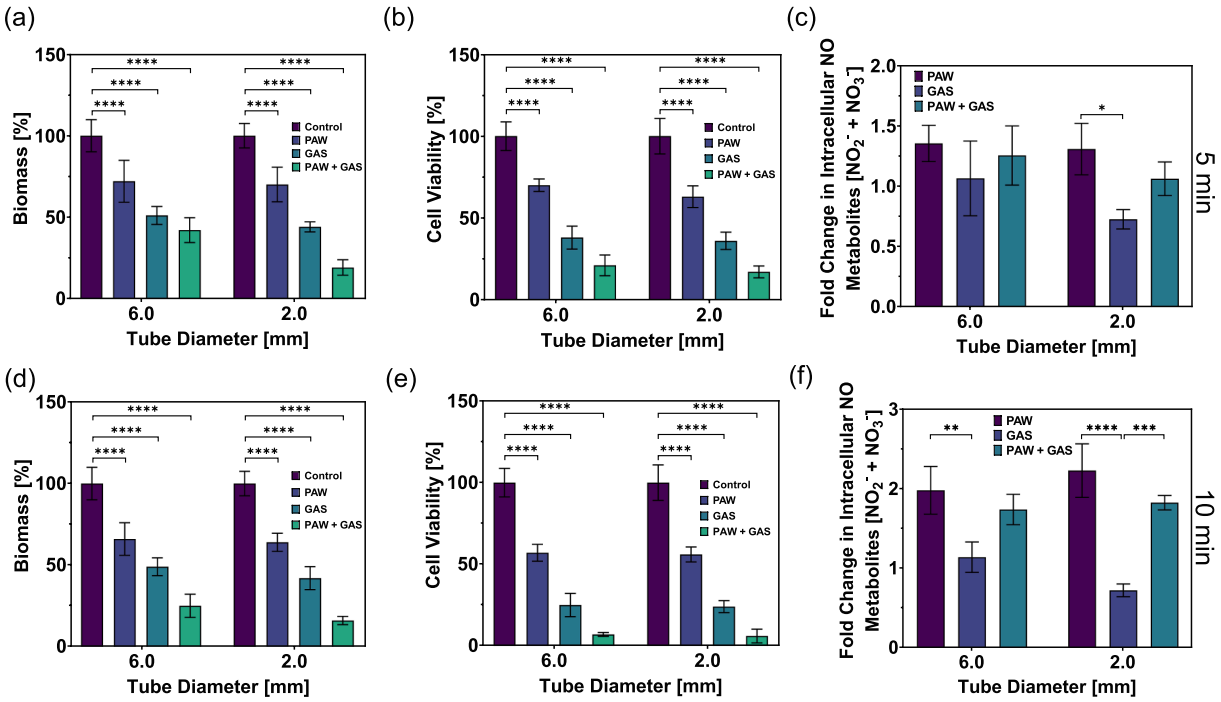

Fig. 6. Influence of plasma treatment on: (a) percentage biomass measured using a crystal violet assay after a 5 min treatment, (b) percentage cell viability measured using an MTT assay after a 5 min treatment time, and (c) fold change in intracellular NO metabolites [NO_2^- and NO_3^-] compared to control in response to 5 minute plasma treatment. With (d), (e), and (f) showing biomass, cell viability and change in NO metabolites for a 10 min plasma exposure, respectively. (For interpretation of the references to colour in this figure legend, the reader is referred to the web version of this article.)

organism for biofilm disinfection [53]. *P. aeruginosa* is an opportunistic pathogen often associated with acute and chronic infections [54]. Its complex biofilms consist of significant amounts of extracellular matrix material [25,55]. Despite this, results have shown the *P. aeruginosa* biofilm had high susceptibility to all plasma treatments. Previous studies have detailed the bacterium's increased susceptibility to RNS-dominated conditions. In summary, the results indicate all methods were capable of significant biofilm reduction, however a combination of PAW + GAS treatment was the most effective. This is consistent with findings shown in Fig. S1, where a 10 min PAW + GAS was most effective and resulted in 5.58, 5.91, 4.60, and 5.01 log reductions in *E. coli*, *S. aureus*, *S. epidermidis* and *P. aeruginosa* biofilms respectively.

3.4. Effect of plasma treatment on mixed species biofilms

While a large proportion of studies are conducted using simplified single species biofilms models as a starting point, they are not fully representative of real-world medical device contamination where the devices are exposed to an array of species within the patient's microbiome [3,4]. Therefore, following confirmation of plasma treatment as an effective method of biofilm reduction, mixed species biofilms were explored. Mixed species biofilms contained *E. coli*, *S. aureus*, *S. epidermidis*, and *P. aeruginosa* strains. Due to the complex nature of mixed species biofilms, it was expected that these would be more resistant to treatment than the single species biofilms [25,56]. The same test piece contamination procedure was followed, with minor adjustments in order to obtain similar starting bacterial concentrations for each strain [17,37]. Disinfection methods were the same as for single species biofilms. Again, the results demonstrated that all plasma treatments were capable of achieving a significant reduction in mixed species biofilms recovered from the test pieces. PAW treatment showed the lowest reduction in biofilm with 2.0 mm test pieces showing a 3.07- and 3.54 log reduction after 5- and 10- min treatment, shown in Fig. 5(a). In test pieces with a larger diameter, log reductions were 2.38, and 2.79 for 5- and 10- min treatment times, respectively. A GAS treatment showed larger log reductions, reaching up to a 4.48 log-reduction after 10 min, displayed in Fig. 5(b). However as shown in Fig. 5(c), a 10 min PAW + GAS treatment was the most effective approach resulting in a 5.45 and 5.72 log reduction in 6.0- and 2.0- mm test pieces, respectively. Results detailed in Fig. S2 highlight that, under certain conditions, a 10 min PAW and GAS treatment offered enhanced antimicrobial performance compared to a 10 min treatment with a commercially available pH buffered peracetic acid commonly used for endoscope disinfection. It is important to note that the disinfection stage of endoscope reprocessing is not expected to remove all biocontamination, hence the need for multiple stages in the AER process [3,5]. As the disinfection process requires the use of harmful chemicals, a fine balance between disinfection and resulting damage to tubing must be struck. There are differing reports of what log reduction is required at the disinfection stage to ensure the lowest risk of human disease transmission, some EN standards require a 5 log reduction and consider this the gold standard in reducing risk as much as possible, while other standards require a 6 log reduction to achieve high-level disinfection [57-60]. Critically, the results presented in this study demonstrate that a 10 min combined PAW + GAS treatment can reach the gold standard disinfection levels of mixed species biofilms, nearing high-level disinfection.

Responses across individual species within the mixed species biofilm are detailed in Fig. 5(d-f). Notably, *P. aeruginosa* single species biofilms showed a higher log reduction than other species, however within the mixed species biofilms growth remained higher than other species. This has been observed in other studies [36]. *S. epidermidis* single species biofilms were the most resistant to plasma treatments, however within the mixed species biofilm environment they exhibited significantly lower growth, particularly following PAW treatment. It has been detailed in various other studies that *P. aeruginosa* thrives in a mixed species environment [61,62]. These results highlight the importance of the complex nature of mixed species biofilms as the bacterial species within are not only responding to outside influence but also working both synergistically and antagonistically with each other.

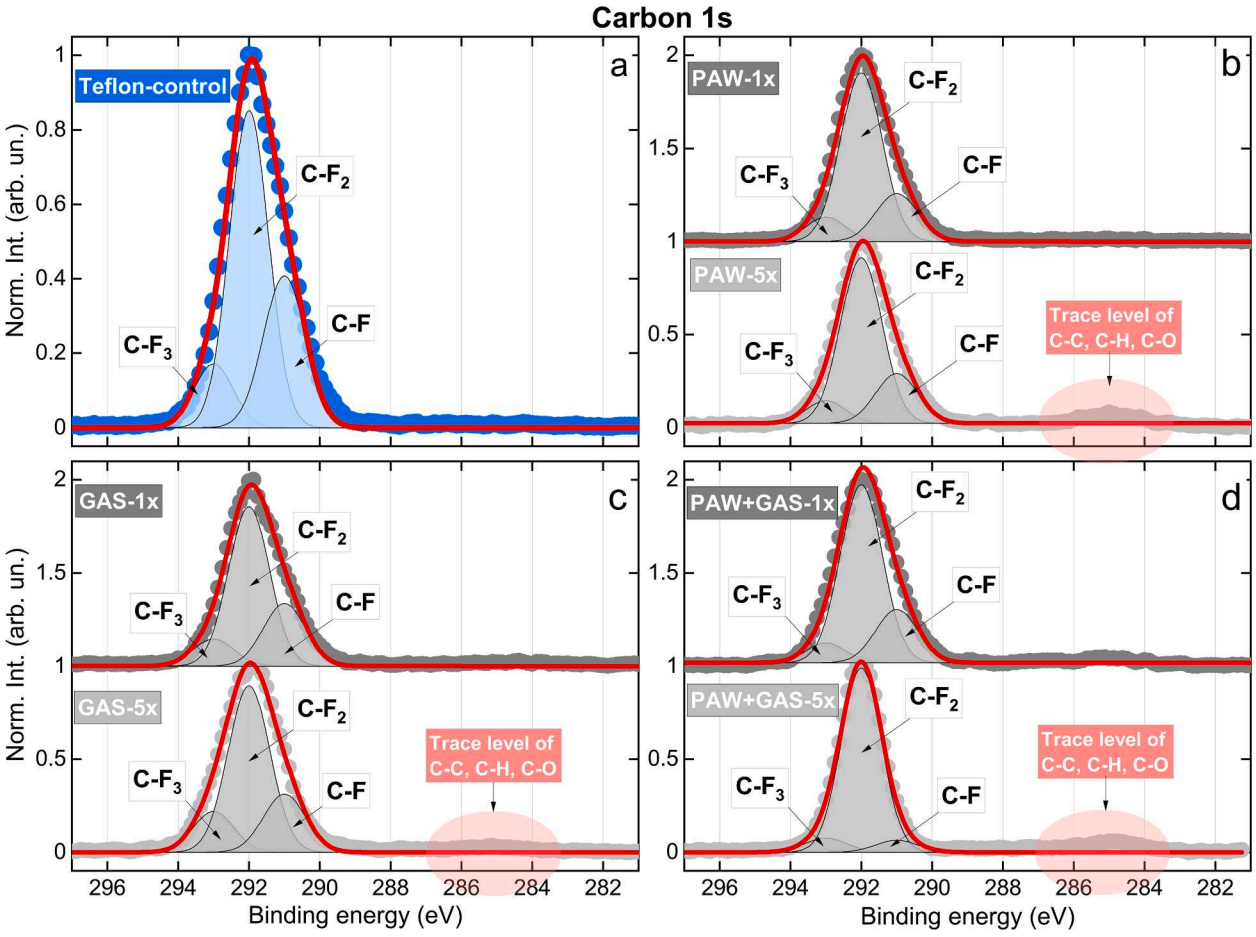

Fig. 7. High-resolution carbon C 1s spectra with corresponding deconvolution of peak components.

3.5. Impact of plasma treatment on biofilm biomass, cell viability, and intracellular nitrogen

The impact of plasma exposure on biofilm biomass, cell viability, and intracellular nitrogen was assessed by various assays. Mixed species biofilms were evaluated after 5- and 10- min plasma disinfection treatments using crystal violet staining, MTT assay, and an intracellular nitrate/nitrite assay. Following plasma treatment, all test pieces had significantly reduced biomass present within the narrow lumens, shown in Fig. 6(a,d). Most notably, 5 min of PAW + GAS treatment resulted in the largest reduction in biomass with a 58% reduction for 6.0 mm test pieces and an 81% reduction in 2.0 mm test pieces. Following 10 min of PAW + GAS treatment biomass reduced by 75% and 84% in test pieces of 6.0 mm and 2.0 mm respectively. While there was a significant reduction in resulting biomass between 5 min and 10 min treatment within the 6.0 mm test pieces, there was no significant difference between 5 min and 10 min PAW + GAS treatment for 2.0 mm test pieces. A GAS plasma treatment resulted in less biofilm biomass than PAW treatment for both 5- and 10- min treatment times; however, decreases in biomass following GAS treatment were not significantly different across treatment times. While PAW showed the lowest reduction in biomass, it can still be noted that the decrease was statistically different from the control and followed a consistent reduction across treatment times. Biomass in this instance takes into account biofilm components and not just bacterial cells [63,64]. While a high bacterial log reduction can be shown, a tailing off of the kill rate could be attributed to the build up of cellular debris resulting in reduced biomass removal and potentially providing protection for active cells below [63,65]. Interestingly, Flynn *et al.* showed that no significant changes in viable cell counts of biofilms grown at 24, 48 and 72 h, however the resulting biomass of the formed biofilms were significantly different [64]. This highlights the need for both log reduction and biomass to be taken into account to provide a full picture of bacterial response to plasma treatments. Fig. 6 (b, e) highlights the impact of all treatments on cell viability. Again PAW + GAS treatment showed the largest reduction in cell viability for both treatment times, reaching a 93% and 96% reduction in cell viability following 10 min of treatment in 6.0- and 2.0- mm test pieces. Interestingly, other studies have shown that despite CAP treatment reducing bacterial population to undetectable levels, metabolic assays still indicated presence of viable cells [66]. Exposure to stress often triggers a switch to a viable but non-culturable state, highlighting the need to not solely rely on log reductions from plate count techniques for an accurate picture of the effect of plasma on biofilms [67]. Due to the high log reduction and large reduction in cell viability being in agreement it suggests a PAW + GAS treatment is sufficiently killing the bacteria within the biofilm. However, lower reductions in biomass may suggest an extra step may still be needed to remove remaining debris, like the brushing step currently used in endoscope reprocessing.

Due to the large presence of RNS within the gas phase effluent and the liquid analysis, intracellular NO (NO_2^- + NO_3^-) was assessed using an intracellular nitrite/nitrate colorimetric assay and shown in Fig. 6(c, f). Fold change in intracellular NO was found to be similar for PAW and PAW + GAS treatments. Following 5 min PAW treatment intracellular NO had a 1.35/1.31 fold increase within test pieces with a diameter of 6.0 and 2.0, and PAW + GAS had a 1.25/1.06 fold increase, showing no significant difference. A 5 min GAS treatment resulted in a lower fold change in intracellular NO, with a 1.06/0.72 fold increase. A 10 min PAW treatment resulted in a 1.98/2.23 fold increase in intracellular NO,

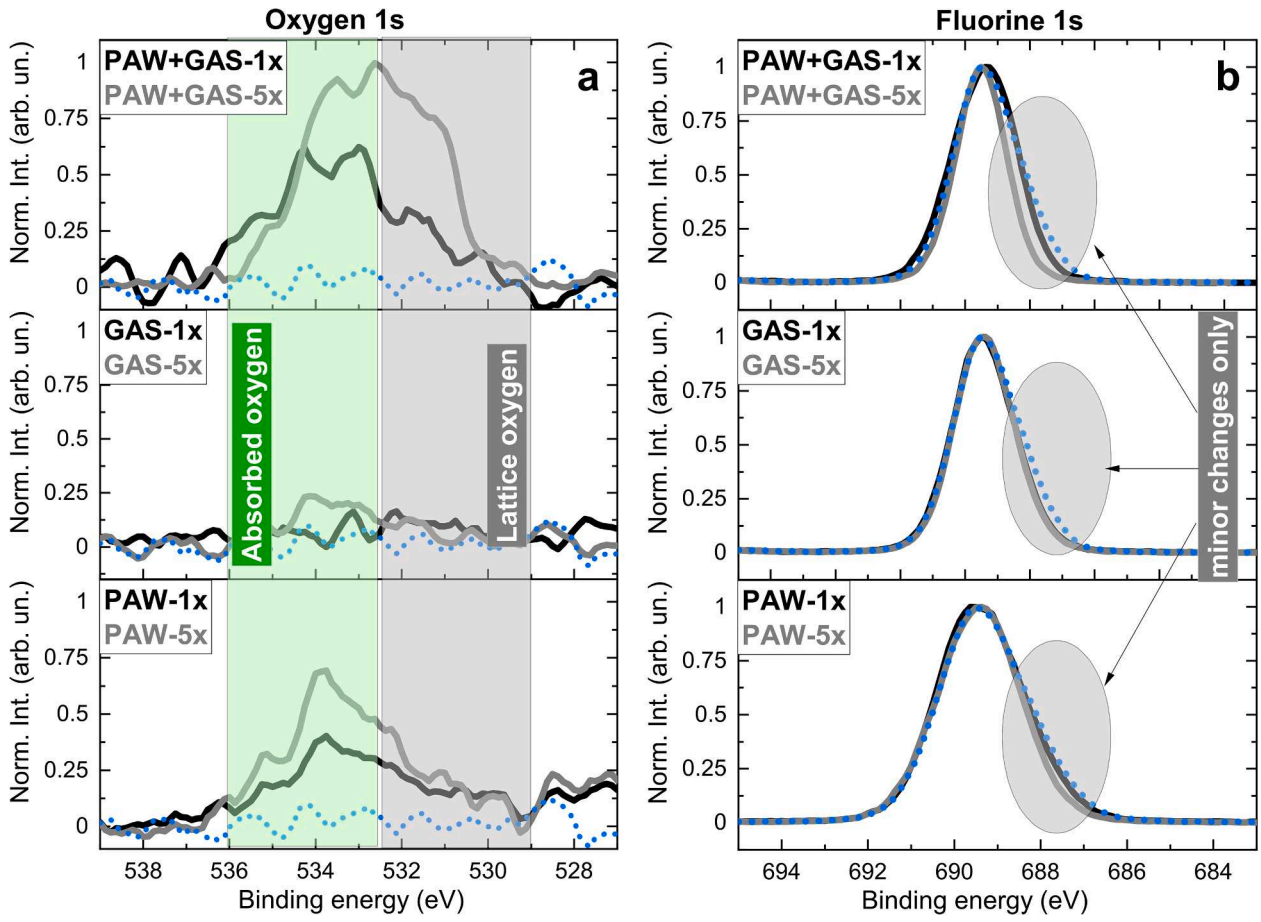

Fig. 8. High-resolution XPS spectra showing oxygen O 1s and fluorine F 1s spectra with corresponding control sample (blue dots). (For interpretation of the references to colour in this figure legend, the reader is referred to the web version of this article.)

and for PAW + GAS a 1.74/1.83 fold increase. A 10 min GAS treatment caused a 1.14/0.72 fold increase, significantly lower than other treatments. It is assumed that the high nitrate/nitrite concentrations within the PAW are responsible for these results. Bacteria possess a variety of defences against RNS used as a response to NO released by mammalian cells during infection; however, these vary across species [68,69]. For example, NO can cause nitrosylation of terminal respiratory cytochromes, however as *S. aureus* can generate ATP via oxidative and substrate-level phosphorylation it is more resistant to NO than bacteria who rely on the electron transport chain for ATP [69]. This could also explain why *S. aureus* proved most resistant to plasma treatments within single species biofilms and showed consistency across treatments within the mixed species biofilm. NO has been found to be involved in biofilm formation, however altering levels of NO can trigger biofilm inhibition and cause dispersal of cells within formed biofilms, thus overcoming the resistant nature of mixed species biofilms and increasing bacterial susceptibility to antimicrobial agents [63,70,71]. Bhatt *et al.* detailed a high log reduction in bacterial biofilms in response to plasma treatment, however most notably they detail plasma treatment caused dispersal of luminal biofilms [72]. Further insight into whether a combination of PAW + GAS treatment triggers biofilm dispersal is needed.

3.6. Influence of plasma treatment on the inner surface of endoscopic test pieces

The influence of plasma treatment on the surface composition and chemical bonding of the endoscopic test pieces was investigated using XPS. Fig. 7(a) shows the C 1s spectra for the endoscopic test pieces, this is a typical spectrum of Teflon and displays no environmentally absorbed oxygen [73,74]. Investigation of the surface composition of plasma treated endoscopic test pieces displayed the characteristic peaks of C, O and F. High resolution C 1s spectra for test pieces treated with PAW, GAS and PAW + GAS are shown in Fig. 7(b-d). For all samples, the dominant C-F_2 bonds are centred at 292 eV with accompanying satellites placed on both sides of the parent peak. For all plasma treatments there were very minor relative peak increases in the C-F_2 peak in comparison to the control. This indicates very minor chemical modifications of the surface saturated bonds. Conversely, C-F and C-F_3 peaks showed a slight decrease in their fitted areas (peak areas detailed in Table S1). For all treated samples there was occurrence of trace levels of C–C/C–H and C-O after 5x plasma treatments, with the peaks for PAW and PAW + GAS treatments being higher than for GAS treatment.

High resolution O 1 s and F 1 s XPS-spectra for control and treated test pieces are shown in Fig. 8. With Fig. 8(a) displaying an increase in the broad peak at ~533 eV for both PAW and PAW + GAS treatments, indicating an increase in absorbed oxygen. It is suggested that this is a result of the endoscopic test pieces coming into contact with O–H present in the water, which explains the lack of peak increase following GAS treatment. It could also be said that it is a result of F-O or C-O binding components, however this is less likely. Fluorine peaks (F 1s) displayed in Fig. 8(b) show a minor unshouldering at the lower energy side related to C-F binding. These results are in good agreement with C 1s fittings mentioned previously. It is also important to note that nitrogen containing compounds were not detected on the endoscopic test pieces suggesting it is unlikely that any nitrates or nitrites were deposited on the surface during the disinfection process. The results indicate practically negligible changes occur to the surface composition regardless of the plasma treatment used and indicate that the surface is not affected or

Table 1
Mean surface roughness obtained from three randomly selected 5 μm × 5 μm scanning areas. Treatment cycles were each 5 min and measurements taken before and after plasma treatment.

	Treatment Cycles	R_a [nm]	
		$\bar{X}$	*sd*
Control	0	21.50	2.62
PAW	1	19.35	1.60
	5	15.62	2.24
GAS	1	27.57	3.01
	5	17.34	4.54
PAW + GAS	1	23.15	3.90
	5	19.23	2.62

functionalised by the disinfection procedure. This is supported by ATR-FTIR absorbance spectra shown in Fig. S3 where no changes were seen to the endoscopic test pieces as a result of plasma treatments. Negligible changes to the surface of the endoscopic test pieces could be attributed to the use of an indirect plasma treatment. Direct plasma systems have previously been shown to cause significant wanted and unwanted chemical changes to the surface [75-77].

3.7. Influence of plasma treatment on endoscopic test piece surface roughness and morphology

The impact of plasma treatment on surface roughness and morphology was examined using AFM. A minimum of three randomly selected areas on the endoscopic test pieces were selected for surface visualisation and calculation of mean surface roughness (R_a). Results are presented as mean value and standard deviation in Table. 1. Control test pieces were found to have an average surface R_a of 21.50 (±2.62) nm. Plasma treatment was carried out 1x 5 min and 5x 5 min to assess changes following multiple uses. Following PAW treatment for 1x 5 min and 5x 5 min the R_a was found to be 19.35 (±1.60) nm and 15.62 (±2.24) nm. Treatment using GAS plasma followed a similar trend, with 1x resulting in the R_a being 27.57 (±3.01) nm and 5x being 17.34 (±4.54) nm. The mean surface roughness for PAW + GAS treatment shows the least variation from the control sample. For 1x the calculated R_a was 23.15 (±3.90) nm and 19.23 (±2.62) nm for 5x PAW + GAS treatment. No significant difference was found.

AFM analysis revealed very minor changes in morphology between the control and plasma treated test pieces, shown in Fig. 9(a-d). Following plasma treatment, no significant changes to the surface roughness and morphology of the test pieces were found. Previous studies have shown that bacterial adherence is influenced by the morphology of a surface, and changes in surface morphology can negatively impact bacterial recolonisation [25,78]. While no significant changes were found, it was important to confirm the impact of plasma treatment on recolonisation. Fig. S4 details microbial recolonisation following multiple PAW + GAS treatment cycles. Results showed recolonisation did not increase, and was in fact significantly lower than control test pieces in 6.0 mm diameter endoscopic test pieces.

4. Conclusion

This study demonstrates that CAP can be used in a two-step approach to effectively disinfect a wide range of pathogens involved in medical device cross-contamination. The results provide a strong basis for further exploration of a multistep CAP treatment as a method for the high-level disinfection of flexible endoscopes. Not only does the use of the combined approach result in significant removal of single species biofilm contamination, it can provide up to a 5.72 log reduction in mixed species biofilms, reaching the gold standard for reducing patient cross-contamination and nearing high-level disinfection levels. However, it is important to note that the nature of the biofilm used in this study can be considered more rigorous than would be typically be used for usual disinfection tests. Critically, the surface composition and roughness of endoscopic test pieces following the two-step disinfection process were assessed and no significant changes were identified, even after multiple disinfection cycles. These findings, combined with an assessment on the ability of bacteria to recolonise the surface, provide encouraging evidence that the two-step CAP based approach is not only effective, but is safe to use on expensive reusable medical devices and its repeated use may even inhibit future biofilm formation. Ultimately, it is clear that the developed approach is viable and warrants further exploration into how it can play a role within automated endoscope reprocessing.

Ethical approval: Not required.

CRediT authorship contribution statement

Naomi Northage: Conceptualization, Methodology, Validation, Formal analysis, Writing – original draft, Visualization. **Stéphane Simon:** Methodology, Investigation. **Vasyl Shvalya:** Investigation, Visualization. **Martina Modic:** Investigation. **Thorsten Juergens:** Resources. **Sascha Eschborn:** Resources. **Malcolm J. Horsburgh:** Supervision. **James L. Walsh:** Conceptualization, Writing – review & editing, Supervision, Funding acquisition.

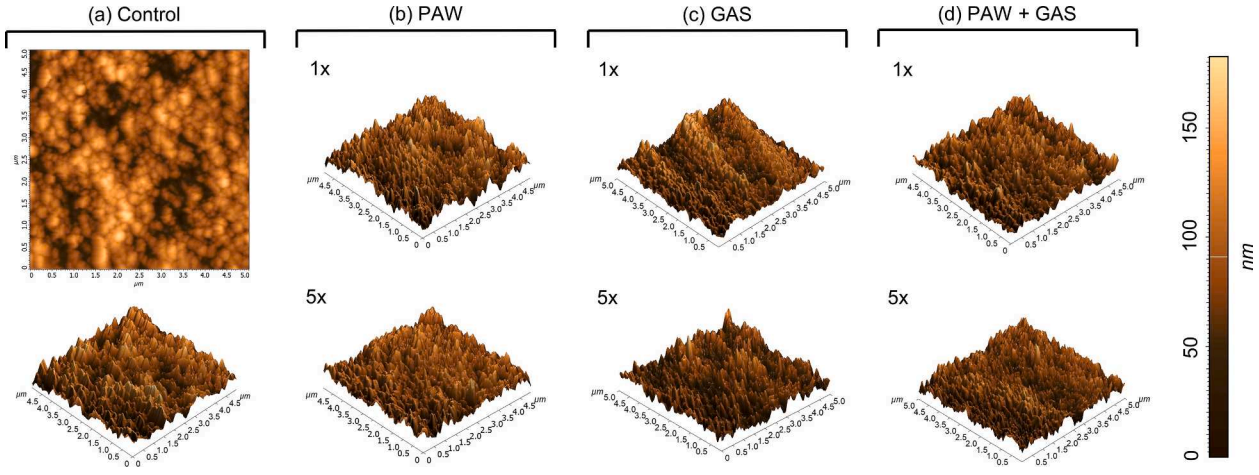

Fig. 9. Representative two- and three- dimensional morphological images of endoscopic test pieces before and after plasma treatment cycles: (a) control, (b) PAW, (c) GAS, and (d) PAW + GAS.

Declaration of Competing Interest

The authors declare the following financial interests/personal relationships which may be considered as potential competing interests: [James Walsh reports equipment, drugs, or supplies was provided by Olympus Winter und Ibe GmbH.].

Data availability

Data will be made available on request.

Acknowledgements

The authors gratefully acknowledge financial support from the Engineering and Physical Sciences Research Council (Projects EP/N021347/1 and EP/S025790/1) and Public Agency for Research Activity of the Republic of Slovenia (ARRS) grants J2-4451 and J2-4490. The authors are thankful to Olympus Surgical Technologies Europe for provision of the endoscopic test materials and pH buffered peracetic acid.

Appendix A. Supplementary material

Supplementary data to this article can be found online at https://doi.org/10.1016/j.apsusc.2023.156936.

References

[1] Gastrointestinal endoscopy: past and future, Gut, vol. 55, pp. 1061-1064, 2006, doi: 10.1136/gut.2005.086371.
[2] J. Kovaleva, Endoscope drying and its pitfalls, J. Hosp. Infect. 97 (4) (Dec. 2017) 319–328, https://doi.org/10.1016/J.JHIN.2017.07.012.
[3] D.B. Nelson, L.F. Muscarella, Transmission of infection during gastrointestinal endoscopy current issues in endoscope reprocessing and infection control during gastrointestinal endoscopy, 2006. [Online]. Available: http://www.wjgnet.com/1007-9327/12/3953.asp.
[4] J. Kovaleva, F.T.M. Peters, H.C. van der Mei Mei, J.E. Degener, Transmission of infection by flexible gastrointestinal endoscopy and bronchoscopy, Clin. Microbiol. Rev. 26(2). Am. Soc. Microbiol. (2013) 230-253. doi: 10.1128/CMR.00085-12.
[5] H.H. Choi, Y.-S. Cho, Endoscopic disinfection in the era of MERS, Clin Endosc 48 (2015) 356–360, https://doi.org/10.5946/ce.2015.48.5.356.
[6] D. Lichtenstein, M.J. Alfa, Cleaning and disinfecting gastrointestinal endoscopy equipment, Clin. Gastrointestinal Endoscopy (2019), https://doi.org/10.1016/b978-0-323-41509-5.00004-9.
[7] K.-W. Chiu, High-level disinfection of gastrointestinal endoscope reprocessing, World J Exp Med 5(1) (2015), doi: 10.5493/wjem.v5.i1.33.
[8] H. Martiny, H. Floss, B. Zühlsdorf, The importance of cleaning for the overall results of processing endoscopes, J. Hosp. Infect. 56 (2004) 16–22, https://doi.org/10.1016/j.jhin.2003.12.027.
[9] A. Gado, B. Ebeid, A. Abdelmohsen, A. Axon, Assurance program, Alex. J. Med. 50 (1) (2019) 7–12, https://doi.org/10.1016/j.ajme.2013.03.001.
[10] Hse, An evaluation of chemical disinfecting agents used in endoscopy suites in the NHS, 2006.
[11] A.B. Akinbobola, N.J. Amaeze, W.G. Mackay, G. Ramage, C. Williams, 'Secondary biofilms' could cause failure of peracetic acid high-level disinfection of endoscopes, J. Hosp. Infect. 107 (2021) 67–75, https://doi.org/10.1016/J.JHIN.2020.09.028.
[12] K.H. Hong, Y.J. Lim, Recent update of gastrointestinal endoscope reprocessing, Clin. Endoscopy 46 (3) (2013) 267–273, https://doi.org/10.5946/ce.2013.46.3.267.
[13] A. Deb, et al., Gastrointestinal endoscopy-associated infections: update on an emerging issue, Dig. Dis. Sci. 67 (2022) 1718–1732, https://doi.org/10.1007/s10620-022-07441-8.
[14] G. Thornhill, M. David, Endoscope-associated infections: a microbiologist's perspective on current technologies, Techniques in Gastrointestinal Endoscopy, vol. 21, no. 4. W.B. Saunders, Oct. 01, 2019. doi: 10.1016/j.tgie.2019.150625.
[15] K. Vickery, Q.D. Ngo, J. Zou, Y.E. Cossart, The effect of multiple cycles of contamination, detergent washing, and disinfection on the development of biofilm in endoscope tubing, Am. J. Infect. Control 37 (6) (2009) 470–475, https://doi.org/10.1016/j.ajic.2008.09.016.
[16] M. Heuvelmans, H.F. Wunderink, H.C. van der Mei, J.F. Monkelbaan, Outbreak investigation of Serratia marcescens neurosurgical site infections associated with a contaminated shaving razors, Antimicrob Resist Infect Control 10 (2020) 171, https://doi.org/10.1186/s13756-021-01037-z.
[17] K. Marion, J. Freney, G. James, E. Bergeron, F.N.R. Renaud, J.W. Costerton, Using an efficient biofilm detaching agent: an essential step for the improvement of endoscope reprocessing protocols, J. Hosp. Infect. 64 (2) (2006) 136–142, https://doi.org/10.1016/j.jhin.2006.06.011.
[18] A.S. Katsigiannis, D.L. Bayliss, J.L. Walsh, Cold plasma for the disinfection of industrial food-contact surfaces: an overview of current status and opportunities, Compr. Rev. Food Sci. Food Saf. 21 (2) (2022) 1086–1124, https://doi.org/10.1111/1541-4337.12885.
[19] G. Busco, E. Robert, N. Chettouh-Hammas, J. M. Pouvesle, and C. Grillon, The emerging potential of cold atmospheric plasma in skin biology, Free Radical Biology and Medicine, vol. 161. Elsevier Inc., pp. 290-304, Dec. 01, 2020. doi: 10.1016/j.freeradbiomed.2020.10.004.
[20] W.L. Hui, V. Perrotti, F. Iaculli, A. Piattelli, A. Quaranta, The emerging role of cold atmospheric plasma in implantology: a review of the literature, Nanomaterials 10 (8) (2020) 1505, https://doi.org/10.3390/nano10081505.
[21] T. Bernhardt et al., Plasma medicine: applications of cold atmospheric pressure plasma in dermatology, 2019, doi: 10.1155/2019/3873928.
[22] A. Chiodi Borges, G. de Morais Gouvêa Lima, T. Mayumi Castaldelli Nishime, A. Vidal Lacerda Gontijo, K. Georgiev Kostov, and C. Yumi Koga-Ito, Amplitude-modulated cold atmospheric pressure plasma jet for treatment of oral candidiasis: In vivo study, 2018, doi: 10.1371/journal.pone.0199832.
[23] F. Theinkom et al., Antibacterial efficacy of cold atmospheric plasma against Enterococcus faecalis planktonic cultures and biofilms in vitro, 2019, doi: 10.1371/journal.pone.0223925.
[24] O. Bunz, et al., Cold atmospheric plasma as antiviral therapy-effect on human herpes simplex virus type 1, J. Gen. Virol. 101 (2020) 208–215, https://doi.org/10.1099/jgv.0.001382.
[25] M. Modic, et al., Targeted plasma functionalization of titanium inhibits polymicrobial biofilm recolonization and stimulates cell function, Appl. Surf. Sci. 487 (2019) 1176–1188, https://doi.org/10.1016/j.apsusc.2019.05.153.
[26] M. Hage, S. Khelissa, H. Akoum, N.-E. Chihib, C. Jama, Cold plasma surface treatments to prevent biofilm formation in food industries and medical sectors 1, 3, doi: 10.1007/s00253-021-11715-y.
[27] M. Risa Vaka et al., Towards the next-generation disinfectant: composition, storability and preservation potential of plasma activated water on baby spinach leaves, 2019, doi: 10.3390/foods8120692.
[28] Kostya (ken) Ostrikov et al., Plasma-activated water: Generation, origin of reactive species and biological applications, J. Phys. D: Appl. Phys. 53(30). Institute of Physics Publishing, Jul. 22, 2020. doi: 10.1088/1361-6463/ab81cf.
[29] S. Simon et al., Influence of potable water origin on the physicochemical and antimicrobial properties of plasma activated water 42 (2022) 377-393. doi: 10.1007/s11090-021-10221-3.
[30] E. Tsoukou, P. Bourke, D. Boehm, Temperature stability and effectiveness of plasma-activated liquids over an 18 months period, Water (Switzerland) 12 (11) (2020) 1–18, https://doi.org/10.3390/w12113021.
[31] M.J. Traylor, et al., Long-term antibacterial efficacy of air plasma-activated water, J Phys D Appl Phys 44 (47) (2011), 472001, https://doi.org/10.1088/0022-3727/44/47/472001.
[32] J. Tan, M. v. Karwe, Inactivation and removal of Enterobacter aerogenes biofilm in a model piping system using plasma-activated water (PAW), Innovative Food Science & Emerging Technologies, vol. 69, p. 102664, May 2021, doi: 10.1016/j.ifset.2021.102664.
[33] A. Mai-Prochnow et al., Interactions of plasma-activated water with biofilms: inactivation, dispersal effects and mechanisms of action, doi: 10.1038/s41522-020-00180-6.
[34] S. Park, W. Choe, C. Jo, Interplay among ozone and nitrogen oxides in air plasmas: rapid change in plasma chemistry, Chem. Eng. J. 352 (2018) 1014–1021, https://doi.org/10.1016/J.CEJ.2018.07.039.
[35] P. Lukes, Plasma Sources Science and Technology Aqueous-phase chemistry and bactericidal effects from an air discharge plasma in contact with water: evidence for the formation of peroxynitrite through a pseudo-second-order post-discharge reaction of H 2 O 2 and HNO 2, 2014, doi: 10.1088/0963-0252/23/1/015019.
[36] M. Modic, N.P. McLeod, J.M. Sutton, J.L. Walsh, Cold atmospheric pressure plasma elimination of clinically important single- and mixed-species biofilms, Int. J. Antimicrob. Agents 49 (3) (2017) 375–378, https://doi.org/10.1016/j.ijantimicag.2016.11.022.
[37] E. Deutschland Gmbh, U. Bäumer, Tests for producing biofilm in Hygiene-Test-Dummies (Teflon tubes), 2016.
[38] R. Dringen, L. Kussmaul, B. Hamprecht, Detoxification of exogenous hydrogen peroxide and organic hydroperoxides by cultured astroglial cells assessed by microtiter plate assay, Brain Res. Protoc. 2 (3) (1998) 223–228, https://doi.org/10.1016/S1385-299X(97)00047-0.
[39] J. A. Reisz, N. Bansal, J. Qian, W. Zhao, C.M. Furdui, Effects of ionizing radiation on biological molecules-mechanisms of damage and emerging methods of detection, doi: 10.1089/ars.2013.5489.
[40] B. Offerhaus et al., Determination of NO densities in a surface dielectric barrier discharge using optical emission spectroscopy, J. Appl. Phys. 126(19) (2019), doi: 10.1063/1.5094894.
[41] D. X. Liu et al., Aqueous reactive species induced by a surface air discharge: Heterogeneous mass transfer and liquid chemistry pathways OPEN, 2016, doi: 10.1038/srep23737.
[42] K. Ikuse, S. Hamaguchi, Roles of the reaction boundary layer and long diffusion of stable reactive nitrogen species (RNS) in plasma-irradiated water as an oxidizing media - Numerical simulation study, Jpn J. Appl. Phys. 61(7) (2022), doi: 10.35848/1347-4065/ac7371.
[43] S. Raud et al., The production of plasma activated water in controlled ambient gases and its impact on cancer cell viability, 41 (2021) 1381-1395, doi: 10.1007/s11090-021-10183-6.
[44] P. Lukes, E. Dolezalova, I. Sisrova, M. Clupek, Aqueous-phase chemistry and bactericidal effects from an air discharge plasma in contact with water: Evidence

for the formation of peroxynitrite through a pseudo-second-order post-discharge reaction of H2O 2 and HNO2, Plasma Sources Sci. Technol. 23(1) (2014), doi: 10.1088/0963-0252/23/1/015019.
[45] G. Bruno, S. Wenske, J.-W. Lackmann, M. Lalk, T. von Woedtke, K. Wende, On the liquid chemistry of the reactive nitrogen species peroxynitrite and nitrogen dioxide generated by physical plasmas, doi: 10.3390/biom10121687.
[46] N. Hojnik, M. Modic, Y. Ni, G. Filipič, U. Cvelbar, J.L. Walsh, Effective fungal spore inactivation with an environmentally friendly approach based on atmospheric pressure air plasma, Environ. Sci. Technol. 53 (4) (2019) 1893–1904, https://doi.org/10.1021/acs.est.8b05386.
[47] J. Chauvin, F. Judée, M. Yousfi, P. Vicendo, N. Merbahi, Analysis of reactive oxygen and nitrogen species generated in three liquid media by low temperature helium plasma jet, doi: 10.1038/s41598-017-04650-4.
[48] A. Mai-Prochnow, et al., Interactions of plasma-activated water with biofilms: inactivation, dispersal effects and mechanisms of action, NPJ Biofilms Microbiomes 7 (1) (2021) 11, https://doi.org/10.1038/s41522-020-00180-6.
[49] F. Vatansever, et al., Antimicrobial strategies centered around reactive oxygen species - bactericidal antibiotics, photodynamic therapy, and beyond, FEMS Microbiol Rev 37 (6) (2013) 955–989, https://doi.org/10.1111/1574-6976.12026.
[50] S.J. Klebanoff, Reactive nitrogen intermediates and antimicrobial activity: role of nitrite, Free Radic. Biol. Med. 14 (4) (1993) 351–360, https://doi.org/10.1016/0891-5849(93)90084-8.
[51] A. Mai-Prochnow, M. Clauson, J. Hong, A.B. Murphy, Gram positive and Gram negative bacteria differ in their sensitivity to cold plasma OPEN, Nat. Publ. Group (2016), https://doi.org/10.1038/srep38610.
[52] T.J. Silhavy, D. Kahne, S. Walker, The Bacterial Cell Envelope, doi: 10.1101/cshperspect.a000414.
[53] Z. Khatoon, C.D. McTiernan, E.J. Suuronen, T.-F. Mah, E.I. Alarcon, E.I. Alarcon Bacterial, Bacterial biofilm formation on implantable devices and approaches to its treatment and prevention, Heliyon 4 (2018) 1067, doi: 10.1016/j.heliyon.2018.
[54] B. Casciaro et al., Inhibition of Pseudomonas aeruginosa biofilm formation and expression of virulence genes by selective epimerization in the peptide Esculentin-1a(1-21)NH 2, doi: 10.1111/febs.14940.
[55] B. Shan Tseng et al., A biofilm matrix-associated protease inhibitor protects pseudomonas aeruginosa from proteolytic attack, 2018, doi: 10.1128/mBio.
[56] L. Fernández, et al., Fighting mixed-species microbial biofilms with cold atmospheric plasma, Front. Microbiol 11 (2020) 1000, https://doi.org/10.3389/fmicb.2020.01000.
[57] A.P. Fraise, European norms for disinfection testing, J. Hosp. Infect. 70 (2008) 8–10, https://doi.org/10.1016/S0195-6701(08)60004-3.
[58] Q. Lin et al., Sanitizing agents for virus inactivation and disinfection, View 1(2) (2020), doi: 10.1002/viw2.16.
[59] B.J. Kovacs, Y.K. Chen, J.D. Kettering, R.M. Aprecio, I. Roy, High-level disinfection of gastrointestinal endoscopes: are current guidelines adequate? Am. J. Gastroenterol. 94 (6) (1999) 1546–1550, https://doi.org/10.1111/j.1572-0241.1999.01142.x.
[60] R.L. Foliente, B.J. Kovacs, R.M. Aprecio, H.J. Bains, J.D. Kettering, Y.K. Chen, Efficacy of high-level disinfectants for reprocessing GI endoscopes in simulated-use testing, Gastrointest Endosc 53 (4) (2001) 456–462, https://doi.org/10.1067/mge.2001.113380.
[61] M. Strous et al., Pseudomonas aeruginosa PAO1 exopolysaccharides are important for mixed species biofilm community development and stress tolerance, 2015, doi: 10.3389/fmicb.2015.00851.
[62] Y. Cheng et al., ARTICLE Population dynamics and transcriptomic responses of Pseudomonas aeruginosa in a complex laboratory microbial community, doi: 10.1038/s41522-018-0076-z.
[63] M. Kostakioti, M. Hadjifrangiskou, S.J. Hultgren, Bacterial biofilms: development, dispersal, and therapeutic strategies in the dawn of the postantibiotic era, doi: 10.1101/cshperspect.a010306.
[64] P. B. Flynn, W. G. Graham, B.F. Gilmore, Acinetobacter baumannii biofilm biomass mediates tolerance to cold plasma, 2019, doi: 10.1111/lam.13122.
[65] R.M. Donlan, J. William Costerton, Biofilms: survival mechanisms of clinically relevant microorganisms, Clin. Microbiol. Rev. 15 (2) (2002) 167–193, https://doi.org/10.1128/CMR.15.2.167-193.2002.
[66] A.D. Patange, J.C. Simpson, J.F. Curtin, C.M. Burgess, P.J. Cullen, B.K. Tiwari, Inactivation efficacy of atmospheric air plasma and airborne acoustic ultrasound against bacterial biofilms, Scientific Reports 11, 2346, 123AD, doi: 10.1038/s41598-021-81977-z.
[67] L. Li et al., The importance of the viable but non-culturable state in human bacterial pathogens, 1982, doi: 10.3389/fmicb.2014.00258.
[68] D.A. Wink, et al., Nitric oxide and redox mechanisms in the immune response, J. Leukoc. Biol 89 (2011) 873–891, https://doi.org/10.1189/jlb.1010550.
[69] F. C. Fang, A. Vázquez-Torres, Reactive nitrogen species in host-bacterial interactions, doi: 10.1016/j.coi.2019.05.008.
[70] D.E. Williams, E.M. Boon, Towards understanding the molecular basis of nitric oxide-regulated group behaviors in pathogenic bacteria, J. Innate Immun. 11 (3) (2019) 205–215, https://doi.org/10.1159/000494740.
[71] N. Barraud, D.J. Hassett, S.-H. Hwang, S.A. Rice, S. Kjelleberg, J.S. Webb, Involvement of nitric oxide in biofilm dispersal of *Pseudomonas aeruginosa*, J. Bacteriol. 188 (21) (2006) 7344–7353, https://doi.org/10.1128/JB.00779-06.
[72] S. Bhatt, et al., Efficacy of low-temperature plasma-activated gas disinfection against biofilm on contaminated GI endoscope channels, Gastrointest. Endosc. 89 (1) (2019) 105–114, https://doi.org/10.1016/j.gie.2018.08.009.
[73] J. Piwowarczyk, R. Jedrzejewski, D. Moszyński, K. Kwiatkowski, A. Niemczyk, J. Baranowska, XPS and FTIR studies of polytetrafluoroethylene thin films obtained by physical methods, Polymers (Basel) 11 (10) (2019) Oct, https://doi.org/10.3390/polym11101629.
[74] G. Cunge, B. Pelissier, O. Joubert, R. Ramos, C. Maurice, New chamber walls conditioning and cleaning strategies to improve the stability of plasma processes, Plasma Sources Sci. Technol. 14 (3) (2005) 599–609, https://doi.org/10.1088/0963-0252/14/3/025.
[75] S.K. Pradhan, M. Jeevitha, S.K. Singh, Plasma cleaning of old Indian coin in H2-Ar atmosphere, Appl Surf Sci 357 (2015) 445–451, https://doi.org/10.1016/J.APSUSC.2015.09.026.
[76] B. Dong, M.S. Driver, I. Emesh, R. Shaviv, J.A. Kelber, Surface chemistry and fundamental limitations on the plasma cleaning of metals, Appl. Surf. Sci. 384 (2016) 294–297, https://doi.org/10.1016/J.APSUSC.2016.05.082.
[77] J. Duchoslav, et al., The effect of plasma treatment on the surface chemistry and structure of ZnMgAl coatings, Appl Surf Sci 504 (2020), 144457, https://doi.org/10.1016/J.APSUSC.2019.144457.
[78] J. Kim et al., Implication of surface properties, bacterial motility, and hydrodynamic conditions on bacterial surface sensing and their initial adhesion, 2021, doi: 10.3389/fbioe.2021.643722.